Dynamic interactive bitwise meta-holography with ultra-high computational and display frame rates

Yuncheng Liu, Ke Xu, Xuhao Fan, Xinger Wang, Xuan Yu, Wei Xiong and Hui Gao

---

Related articles

Crosstalk-free achromatic full Stokes imaging polarimetry metasurface enabled by polarization-dependent phase optimization

Yaxin Zhang, Mingbo Pu, Jinjin Jin, Xinjian Lu, Yinghui Guo, Jixiang Cai, Fei Zhang, Yingli Ha, Qiong He, Mingfeng Xu, Xiong Li, Xiaoliang Ma, Xiangang Luo

Opto-Electronic Advances   2022   **5**, 220058   doi: 10.29026/oea.2022.220058

Multi-foci metalens for spectra and polarization ellipticity recognition and reconstruction

Hui Gao, Xuhao Fan, Yuxi Wang, Yuncheng Liu, Xinger Wang, Ke Xu, Leimin Deng, Cheng Zeng, Tingan Li, Jinsong Xia, Wei Xiong

Opto-Electronic Science   2023   **2**, 220026   doi: 10.29026/oes.2023.220026

Graphene-empowered dynamic metasurfaces and metadevices

Chao Zeng, Hua Lu, Dong Mao, Yueqing Du, He Hua, Wei Zhao, Jianlin Zhao

Opto-Electronic Advances   2022   **5**, 200098   doi: 10.29026/oea.2022.200098

Time-sequential color code division multiplexing holographic display with metasurface

Xin Li, Qinmiao Chen, Xue Zhang, Ruizhe Zhao, Shumin Xiao, Yongtian Wang, Lingling Huang

Opto-Electronic Advances   2023   **6**, 220060   doi: 10.29026/oea.2023.220060

More related article in Opto-Electronic Journals Group website

---

QEA | Opto-Electronic
Advances

http://www.oejournal.org/oea

OE_Journal   @OptoElectronAdv

Dynamic interactive bitwise meta-holography with ultra-high computational and display frame rates

Yuncheng Liu[1†], Ke Xu[1†], Xuhao Fan[1], Xinger Wang[1], Xuan Yu[1], Wei Xiong[1,2]* and Hui Gao[1,2]*

Interactive holography offers unmatched levels of immersion and user engagement in the field of future display. Despite of the substantial progress has been made in dynamic meta-holography, the realization of real-time, highly smooth interactive holography remains a significant challenge due to the computational and display frame rate limitations. In this study, we introduced a dynamic interactive bitwise meta-holography with ultra-high computational and display frame rates. To our knowledge, this is the first reported practical dynamic interactive metasurface holographic system. We spatially divided the metasurface device into multiple distinct channels, each projecting a reconstructed sub-pattern. The switching states of these channels were mapped to bitwise operations on a set of bit values, which avoids complex hologram computations, enabling an ultra-high computational frame rate. Our approach achieves a computational frame rate of 800 kHz and a display frame rate of 23 kHz on a low-power Raspberry Pi computational platform. According to this methodology, we demonstrated an interactive dynamic holographic Tetris game system that allows interactive gameplay, color display, and on-the-fly hologram creation. Our technology presents an inspiration for advanced dynamic meta-holography, which is promising for a broad range of applications including advanced human-computer interaction, real-time 3D visualization, and next-generation virtual and augmented reality systems.

Keywords: interactive display; meta-holography; bitwise operation; ultra-high frame rate

Introduction

Computer-generated holography (CGH), combining holography with computer technology, enables the dynamic reconstruction of virtual objects, and has been widely used in diverse sectors including 3D display[1], optical information storage[2] and processing[3], entertainment[4], and encryption[5,6].

However, the reliance on devices like spatial light modulator (SLM)[7] and the digital micro-mirror device (DMD)[8] in traditional CGH systems has resulted in intrinsic display limitations such as a small field of view (FOV) and multiple orders of diffraction[9]. Recently, metasurfaces[10], composed of numerous subwavelength nanostructures, have demonstrated remarkable capabilities in modulating electromagnetic waves (EM). By introducing abrupt changes in EM wave properties including

[1]Wuhan National Laboratory for Optoelectronics and School of Optical and Electronic Information, Huazhong University of Science and Technology, Wuhan 430074, China; [2]Optics Valley Laboratory, Wuhan 430074, China.
†These authors contributed equally to this work.
*Correspondence: W Xiong, E-mail: weixiong@hust.edu.cn; H Gao, E-mail: gaohui_wnlo@hust.edu.cn

amplitude, phase, and polarization[10], meta-holography has made significant advancements in terms of large FOV[11,12], achromatic imaging[13], color display[14,15], information capacity expansion[16], multi-dimensional multiplexing[17], and more, thereby becoming a potent tool for dynamic holography.

Dynamic meta-holography typically employs two methods: active and multiplexed schemes. Active schemes manipulate the basic properties of the unit structure using active materials like phase change materials[18,19], two-dimensional (2D) materials[20], and various stimuli such as electrical[21,22], chemical[6,23], mechanical[24], and environmental stimuli[25]. On the other hand, multiplexed schemes utilize the combination of static metasurfaces and dynamic modulation of the incident light field properties, such as incident angles[26], polarization states[27,28], orbital angular momentum (OAM)[29], space channel[9], to display different holograms. Despite dynamic meta-holography's notable progress, it is still challenging to achieve real-time fluency to unlock more advanced functionalities in human-computer interaction and light field control systems responding to an external environment.

The key to high fluency in holography lies in the attainment of high computational and display frame rates. Computational frame rates, referring to the speed of data computation, processing, and preparation for display, ensure that the system can calculate the required content in real time. Many current schemes depend heavily on the continuous computation of the Fast Fourier Transform (FFT) one or more times and loading it onto the SLM/DMD. This often requires specialized computing units such as GPUs[30,31] to meet the high-speed refresh demands, making computational power and energy consumption significant limiting factors for large-scale applications. Display frame rates, on the other hand, referring to the speed at which a display device can refresh and present new contents. Active schemes for dynamically modulating metasurface devices and multiplexed schemes employing SLMs as dynamic refresh devices are difficult to attain high display frame rates, which affects the smoothness and dynamism of the visual content.

In this paper, we propose a bitwise meta-holography (Bit-MH) technology designed to achieve dynamic interactive holography with high computational and display frame rates. We spatially partition the display function of the metasurface into distinct channels with space channel multiplexing technology, each projecting a recon-

structed sub-pattern. Efficient dynamic refreshing is achieved by mapping the switching states of the channels to a set of bit values and subsequently controlling the state of the channels via bitwise operations. Tests conducted on the computational platform utilized in this study resulted in a maximum computational frame rate of up to 800 kHz, and concurrently, the DMD used allowed for a maximum display frame rate of up to 23 kHz. As a proof of concept, we constructed an interactive holographic game system for the typical Tetris game in the visible region. Our design enables efficient dynamic updating of the hologram and allows interaction with external inputs. To our knowledge, this is the first demonstration of a practical interactive meta-holography system. We believe that the effective and programmable Bit-MH method can pave the way towards the realization of the seamlessly interactive holographic system.

Materials and methods

The design principle of Bit-MH

Our concept of bitwise meta-holography involves encoding and mapping the dynamic update process of the hologram as bitwise operations on a bit set. This technique permits efficient and unrestricted manipulation of the dynamic state of the hologram, circumventing any complex calculations such as Gerchberg-Saxton (G-S) iterative algorithms[32] required for phase hologram computation. Benefiting from the high efficiency of bitwise operations, our approach allows for the high-speed execution of the dynamic refresh process.

In our design, the display functionality of the metasurface device is compartmentalized into multiple distinct channels, each of which projects an individual reconstructed sub-pattern, and the final displayed reconstructed image is composed of sub-patterns from all activated channels together. Dynamic refresh is achieved by selectively turning these channels on or off. The switching state of each channel is encoded as a bit value, and the collective states of all channels are consolidated into a bit set. Efficient dynamic refreshing can be achieved by performing bitwise operations on this bit set.

Since our scheme aims to control the states of multiple channels efficiently, the division of channels can be achieved via techniques such as space channel multiplexing[9] and OAM channel multiplexing[29]. In this paper, we predominantly employed space channel multiplexing to spatially divide the metasurface device into channel

regions with different sizes, positions, and display functions. A conceptual schematic of the spatial division and selective control of the divided channel area is shown in Fig. 1(a) and 1(b). The DMD is used to dynamically modulate the incident light at high speed, thereby controlling the switching states of channels in different positions. The simple binary control pattern loaded onto the DMD is continuously updated based on these bit values (e.g., bit 0 indicates 'off' and displays black, while bit 1 indicates 'on' and displays white). The overall architecture of the interactive holographic gaming system used to demonstrate our bitwise dynamic meta-holography is
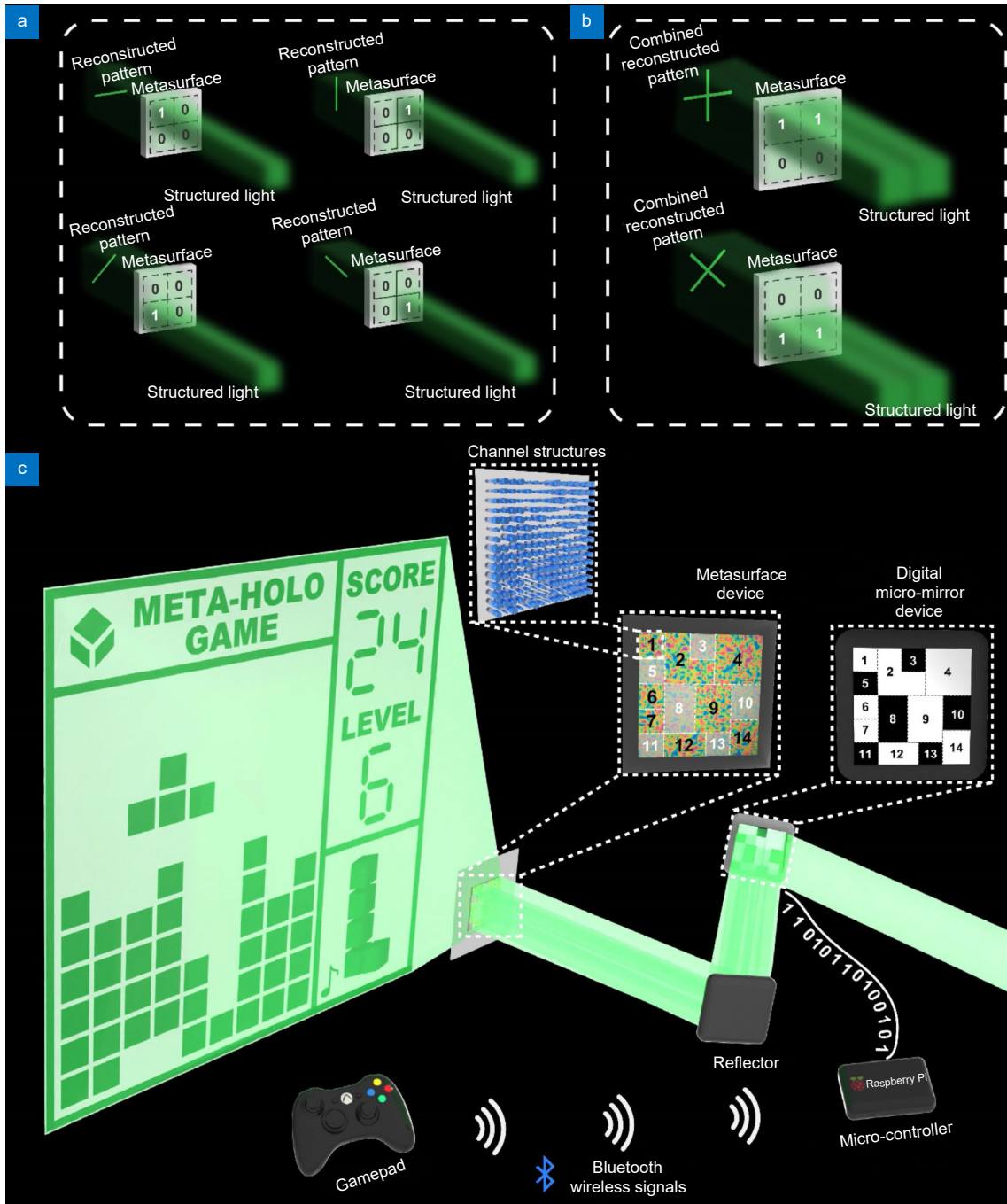

Fig. 1 | Schematic diagram of the channel division concept of Bit-MH and the system for implementing interactive holographic games. The numbers and box lines are added to indicate the channel area; states 0 and 1 indicate corresponding position channel off and on, respectively. (**a**) Schematic of the concept of space channel division and the independent projection of each channel. (**b**) Schematic of selective turn-on channels for combined display. (**c**) Schematic diagram of the architecture of the interactive dynamic metasurface holographic game system. On the DMD, black indicates off, and white indicates on; on the metasurface device, the darker area indicates not being turned on.

shown in Fig. 1(c). It also incorporates a Bluetooth wireless gamepad controller for receiving dynamic control input from the user and a low-power embedded microcontroller for computational and device interconnectivity purposes.

In traditional dynamic holography, the hologram update process relies on the continuous usage of the FFT algorithm to compute the hologram that's loaded onto a dynamic refresh device such as a DMD. This method necessitates the computation of the entire image each time, resulting in a time complexity of up to $O\left(M \cdot N \cdot \log(M \cdot N)\right)$ (the time complexity of the FFT algorithm) per computation, where M and N represent the number of pixels in the rows and columns of the target image, respectively.

Our approach segregates the hologram into K sub-holograms (typically, K is considerably smaller than the number of image pixels $M \cdot N$), so the time complexity for managing the display state of all sub-holograms is $O\left(K\right)$. Our bitwise algorithm exhibits linear time complexity, which is a significant improvement over the square time complexity characteristic of traditional methods. Given that, in reality, not all holograms need to be updated, and each region on the binary control pattern fed to the DMD is independent, we are permitted to make on-demand adjustments each time. Our bitwise operation method swiftly and easily identifies the altered parts between two states via an exclusive OR operation, enabling us to compute an update mask to direct the next control pattern generation strategy. Figure 2 illustrates the core algorithm differences between our Bit-MH and traditional Fourier-based dynamic holography for updating the hologram.

To compare the computational time complexities of two algorithms directly, we executed benchmark measurements on this demonstration platform focusing on computational frame rate generation speed with 600 × 600 pixels image. The computational frame rate generation speed of our method can reach up to 800 kHz, while the single Fourier transform can achieve approximately 30 Hz. On our computing platform, our methodology can enhance the computational frame rate by more than about 10^4 times. Detailed benchmark measurement specifics can be found Supplementary information Section 1. The benchmark testing aimed to highlight the performance disparity between our bitwise algorithm and the traditional Fourier-based algorithms (e.g., G-S iterative optimization algorithm), during the pivotal phase of

hologram generation in holographic display systems. Moreover, the dynamic refresh device in our system, the DMD (Texas Instruments, DLP9500), could provide a display frame rate of up to 23 kHz, empowering our system to achieve high-performance time-sequential cycle-based color display[33] and refined grayscale display.

The design and setup of the interactive Tetris holographic game system

For the purpose of demonstrating Bit-MH actually, we designed and constructed a polarization-insensitive dielectric metasurface device that operates in transmission mode within the visible light band for an interactive Tetris game system.

We chose a silicon nitride nanopillar with a circular cross-section with different radii and 700 nm height. Each nanopillar is located on a silica square substrate of 440 nm period and is illustrated in Fig. 3(a). The radii of nanostructures vary from 61 nm to 153 nm. The electromagnetic response characteristics of nanopillars of different sizes under the incident light with the wavelength of 532 nm were simulated with the finite-difference time-domain (FDTD) method, and we chose eight radii for fabrication. The amount of phase modulation provided by selected nanopillars can cover the whole 2π range, while all nanopillars had high transmittance (Fig. 3(b)).

Finally, we fabricated our metasurface device according to the designed geometries of nanopillars using electron beam lithography (EBL). The optical image of the processed device characterized by the confocal laser scanning microscope (CLSM) is shown in Fig. 3(c). Additionally, the image of a local part of the device characterized by scanning electron microscopy (SEM) is depicted in Fig. 3(d).

To satisfy the dynamic and rich display requirements of the interactive game, we have carefully designed and divided the functions of the different channels. The S channels, which consistently display throughout the game, were termed static channels; the C channels, which cyclically display a set of patterns, were referred to as cyclic channels; and the M channels, which display according to the game state, were called multiplexed channels. In an actual game process, all channels can supply up to $S^0 + C^1 + 2^M$ different effective frames. However, all channels in our design were programmable, allowing for a maximum of up to 2^{S+C+M} different theoretical frames.
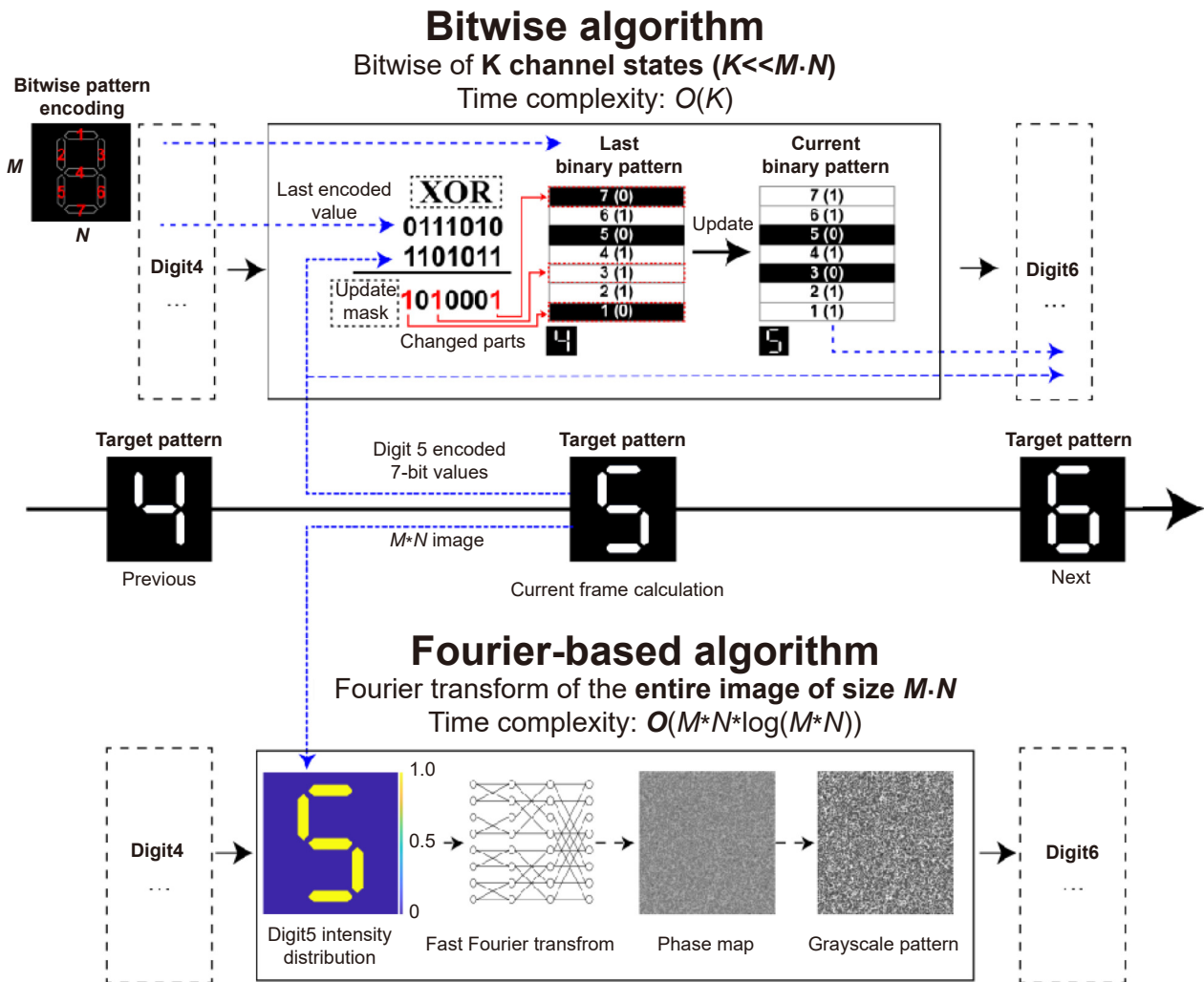
Fig. 2 | Schematic comparison diagram between the bitwise dynamic holography algorithm and the traditional Fourier-based dynamic holography algorithm. For simplicity, a 7-bit digit tube is used as the target image; in our algorithm, the bit values 1 and 0 indicate that the corresponding channels are on and off, respectively; in the binary control image, white and black indicate that part of the channel is on and off, respectively; the box lines in the binary image are used to distinguish the different channels clearly and do not indicate other information. In the update mask of the bitwise algorithm, 0 and 1 respectively indicate that the channel at the corresponding position needs to be flipped or remain unchanged.

We have designed 144 channel regions with varying functions for the Tetris game (The size of the hologram was 3000 rows and 3000 columns of pixels). The division and arrangement of the channels with diverse shapes and size proportions across the entire device are illustrated in Fig. 4(a). We compensated the intensity of the reconstructed pattern at the edge position by adjusting the device region area of different types of channel regions. Furthermore, we made pre-compensation for pattern distortion, ensuring that reconstructed patterns on the flat screen always matched the target pattern. Detailed descriptions of distortion compensation can be found in Supplementary information Section 2. The number of channels largely depends on the intended ap-

plication scenario. In particular, the number of channels correlates with both the intricacy of the reconstructed pattern and the complexity of its motion trajectory. As the desired reconstructed pattern becomes more intricate and its motion trajectory more detailed, there tends to be an increase in the number of allocated channels. Detailed analysis and discussion are provided in Supplementary information Section 3.

In our designed Tetris game, the No. 24 channel was a static channel displaying the main game scene with static borders and texts ($S=1$); channels No. 25 to 33 were cyclic channels that switched and refreshed at a fixed frequency to display a rotating cube ($C=9$); the rest of the 134 channels were multiplexed channels ($M=134$).
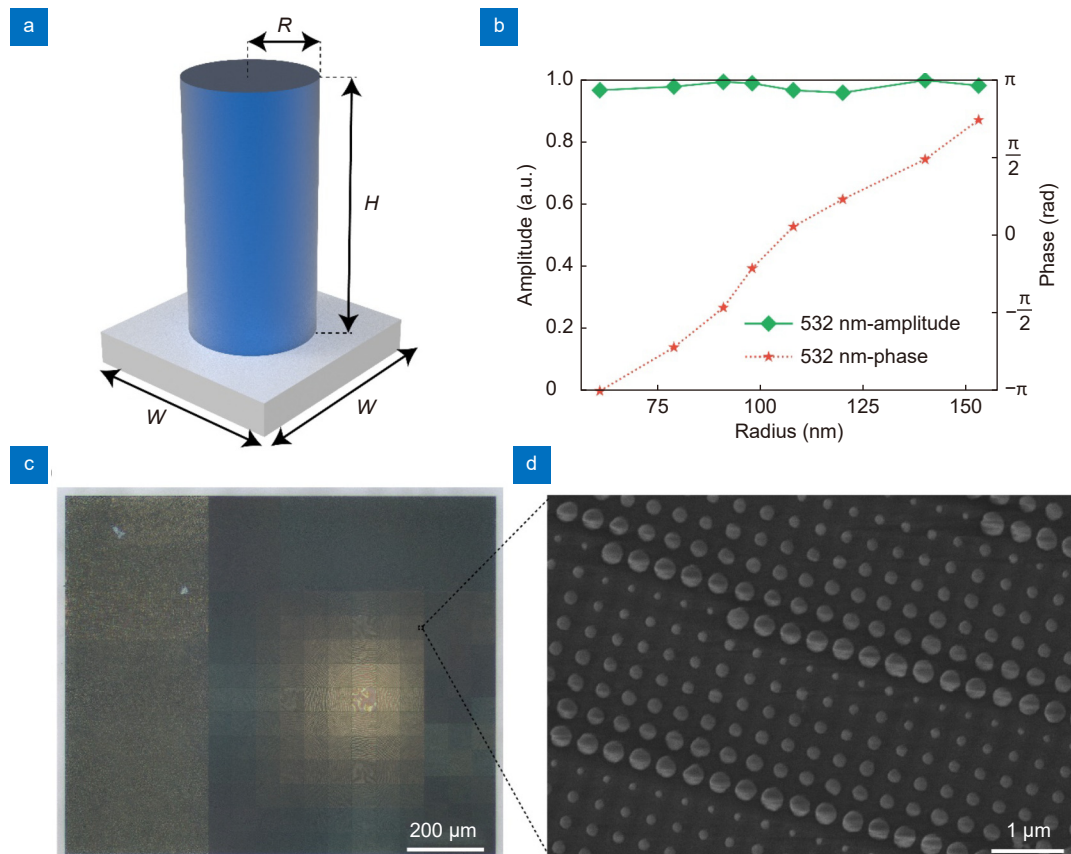
Fig. 3 | Design scheme of cylindric nanopillar with varying radii and same height. (**a**) Geometric parameters of the nanocylinder located in the center of the square lattice, W is the side length of the square lattice, and R and H are the radius and height of the nanocylinder, respectively. (**b**) Results of parameter sweep for the parameter range of R from 55 nm to 160 nm for W = 440 nm, H = 700 nm, and λ = 532 nm. Marked in the figure is the amount of amplitude and phase modulation provided by the selected nanopillars. (**c**) Characterization results of the CLSM of the device; The block-by-block partitions are different channel areas, and the detailed design is described in a later section. (**d**) Characterization results of the SEM of one local part of the device.

Therefore, the design can achieve theoretical frame number $2^{S+C+M} = 2^{144}$, and effective frame number $S^0 + C^1 + 2^M = 1 + 9 + 2^{134}$. Within the multiplexed channels, the central channel array of 11 rows and 9 columns displayed a basic squares array, showcasing the main game canvas; To the right, a portion of the channel array combined into a 2-digit digital tube, displaying the current game score, and another section combined into a 1-bit digital tube, displaying the current game level. Channel No. 34 flashed a music logo in rhythm with the music. Channels No. 134 to 141 were used to display a preview of the block that will appear next. Different channels' projection patterns and positions were detailed and visually represented in Fig. 4(b) and Fig. 4(c).

We utilize the DMD to produce the structured light field, governing the opening states of channel regions, thus there's no limitation to channel's shape. For simplicity, while preserving the study's generality, we opted for a predominantly rectangular channel shape.

The control program running on the low-power embedded platform (Raspberry Pi 4b, 64-bit Raspbian operating system) was developed using C++ programming language, detailed software design and development contents are described Supplementary information Section 4. A regular gamepad (Microsoft Xbox wireless controller) was employed in communicating with the microcontroller (Raspberry Pi 4b, Raspberry Pi Foundation, UK) via a standard Bluetooth communication interface.

In the game process, when a control signal from the gamepad was received, the button identifier was decoded and obtained by the microcontroller. This identifier was then mapped to game action, such as block movement or rotation. Subsequent to the execution of the control operation, the current game states were verified, and the score and level information were updated. All necessary information was immediately encoded into the bit set of game states.

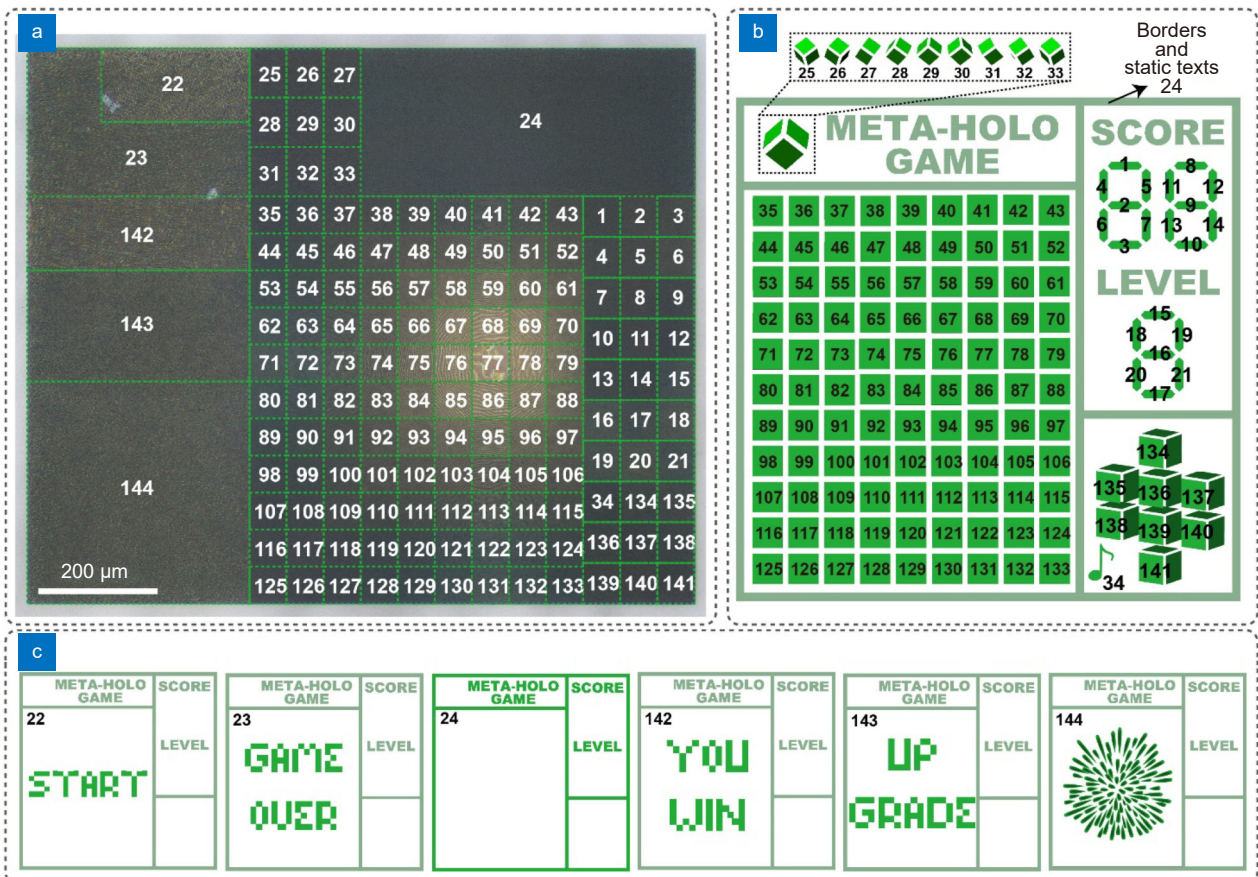The DMD control module was concurrently running

Fig. 4 | Schematic diagram of arrangements, size, and display functions of the channels on the device for Tetris game. (**a**) The arrangement and size of channels on the overall designed device, which were marked based on the characterization result image of the metasurface device using CLSM. The numbers indicate the corresponding numbers of the channels. (**b**) Projection patterns from different channels that do not overlap when displayed. Static channel No. 24 display the fixed border and texts; cyclic channels No. 25 to 33 correspond to different poses of a rotating square, and opening these channels, in turn, realizes a dynamic pattern of rotating squares; cyclic channel No. 34 corresponds to a flashing music logo; multiplexed channels No. 35 to 133 are arrays of squares that form the main game canvas; multiplexed channels No. 1 to 21 and No. 134 to 141 project the digit tubes and simple array of squares illustrated on the right, respectively. (**c**) The text or pattern projection which was displayed in the center. To avoid possible mutual occlusion of patterns displayed in the same area, the text and patterns that would be projected in the center of the main scene are shown separately, corresponding to the (a) diagram, actual holograms of multiplexed channels No. 22 ("START" text), 23 ("GAME OVER" text), 24 (the static borders and texts), 35 to 133 (square array in the main game canvas), 142 ("YOU WIN" text), 143 ("UPGRADE" text), 144 (fireworks pattern), respectively; for a clearer presentation, the static border is always displayed (channel numbered 24).

in the background, where the channel states were read, and the corresponding compact binary control pattern was rendered. This pattern was then written to the standard HDMI output terminal of the microcontroller for the transmission of control data to the DMD, affecting the modulation of the incident light field. This process was continuously executed in a high-speed loop, ensuring constant response to user input. Benefiting from our bitwise dynamic meta-holography technology, game systems that require high computational frame rates and display frames could be operated even on a low-power computing platform.

Results and discussion

We further demonstrate our interactive holographic game system based on Bit-MH through an actual experimental system. To our knowledge, this is the first demonstration of a practical interactive meta-holography system. The system's basic components were, in order, the laser light source, the DMD, the metasurface device, and the requisite optical components. The schematic diagram of the optical system can be found in Supplementary information Section 5 (in Fig. S6). In addition to the continuous execution of the game process, the control program had the ability to enter debug mode,

allowing for arbitrary selection and toggling of several channels' on or off states.

For a more straightforward illustration, we began by freely manipulating the on/off states of channels in debug mode to display a static pattern composed of independent or combined reconstructed sub-patterns from different channels. A 532 nm laser was employed as the light source. We added dark gaps around each channel through the control program to suppress inter-channel crosstalk.

We activated a single channel indicating clearance fireworks to exhibit an independent sub-patterns, as shown in Fig. 5(a). We then played a Tetris game with a regular gamepad with the holographic display system. The rules and game logic were consistent with traditional Tetris. In Fig. 5(b), we showed a frame during the actual operational game with a gamepad and the switching state of the channel in that state to demonstrate the ability to combine displays by controlling multiple channels simultaneously.

In Fig. 5(c), we demonstrated four extracted scenes from the continuous gameplay. In Supplementary information Section 7, we provided three videos, two showing the complete game-over process, game clearance, and the dynamic DMD control pattern of the corresponding channel states, and another video
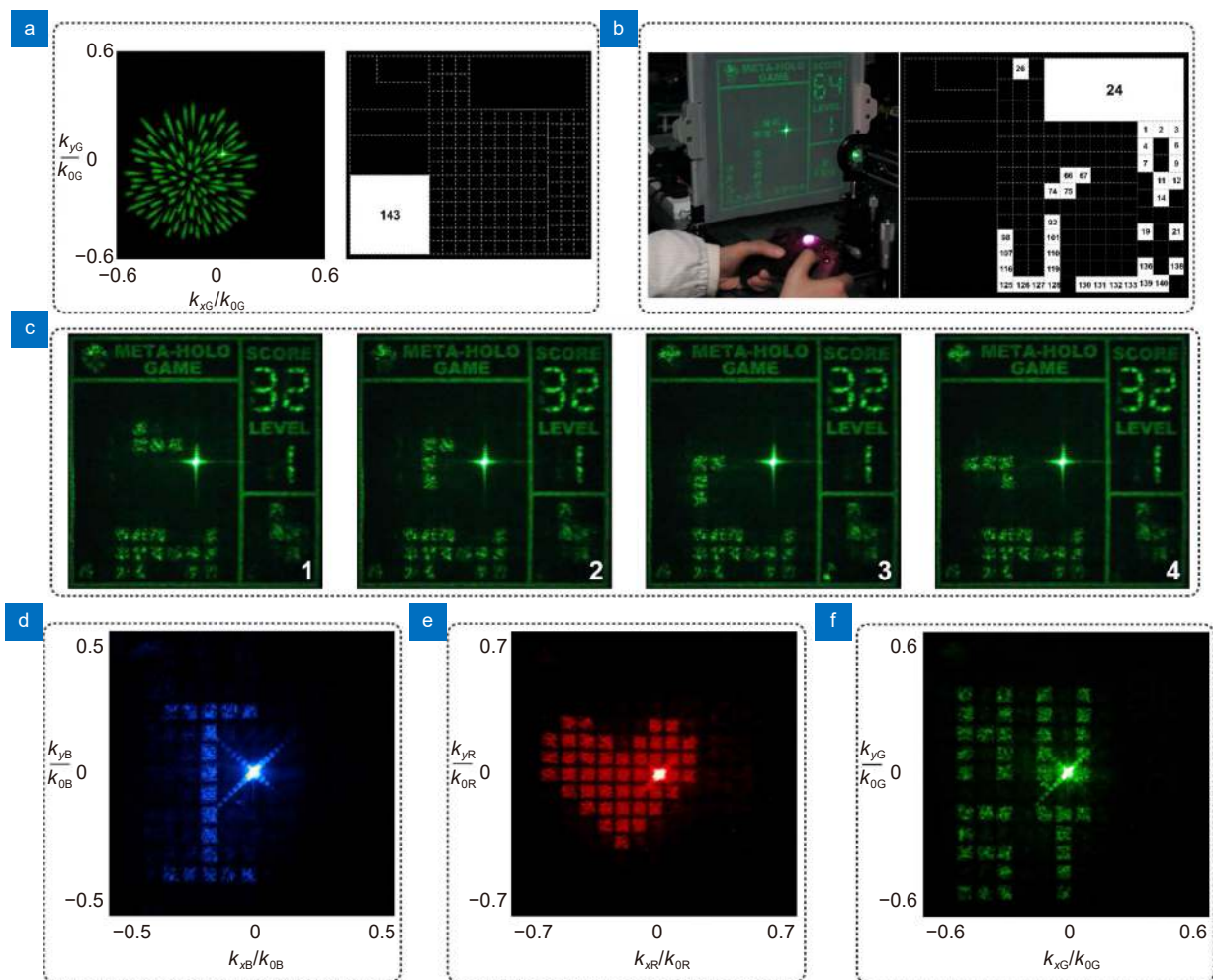

Fig. 5 | Experimental reconstructed patterns results at 473 nm, 532 nm, and 633 nm wavelength with partial channels turned on. In the coordinate axes, k_0 represents the wave vector, and k_x and k_y represent the spatial frequencies in the x and y directions, respectively. k_0 and k_x and k_y at 633 nm, 532 nm, and 573 nm use the corner markers of R, G, and B, respectively. In (**a**) and (**b**), The left side of each subgraph is the pattern and the right side is the diagram of the corresponding channel switching state; black and white refer to the channel close and open, respectively; some spacings are added around channels for clear presentation. (a) The reconstructed pattern of the fireworks. (b) A frame extracted from a game played via a gamepad. (**c**) The extracted stages of the actual playing game. Each of these four frames indicates continuous progress. (**d**) The on-the-fly created text uppercase letter 'I' symbol pattern result at 473 nm wavelength. (**e**) The on-the-fly created heart pattern result at 633 nm. (**f**) The on-the-fly created "HUST" text pattern result at 532 nm.

demonstrating the gameplay process using a gamepad. We believe these three videos visually and efficiently present all the design elements described in the previous section and a seamless interaction process of our holographic game system.

Furthermore, our scheme can enable color display and the real-time combination of basic sub-patterns. The capability of the Bit-MH allowed us to efficiently manipulate different channels simultaneously, which, in addition to the interactive game demonstrated earlier, allowed for the flexible combination of different sub-patterns to improvise unplanned patterns.

To exemplify this, we used the array of squares in the main game scene area to construct more complex patterns composed of basic squares independent of the game and without predefinition. In the debug mode of our control program, we activated the corresponding channels based on the content of the temporarily conceived pattern, immediately generating the desired pattern. We displayed a blue uppercase text 'I' text pattern at 473 nm, a red heart pattern at 633 nm, and a "HUST" text pattern of the school logo in green at 532 nm, as shown in Fig. 5(d–f), respectively. It's important to emphasize that these complex patterns created on-the-fly are not constrained to manual construction using our control program; they can be generated dynamically, based entirely on external input control signals.

Finally, we employed a power meter to measure the optical power impinging upon the entire metasurface (P_{in}), the power of the light transmitted from the metasurface (P_{t}), and the optical power of the unmodulated laser beam (zero-order light) (P_{zero}). The overall efficiency is defined as $Efficiency = (P_{\text{t}}/P_{\text{in}}) \times (1 - P_{\text{zero}}/P_{\text{t}})$. Based on this, we obtained the overall experimental efficiency to be 67.02% at 633 nm, 61.18% at 532 nm, and 51.54% at 473 nm, respectively.

Experimental results validated that our bitwise dynamic meta-holography scheme offers the high computational and display frame rates required by interactive holographic systems, for instance, and retains substantial manipulation flexibility.

Conclusions

In this paper, we introduced a dynamic interactive bitwise meta-holography that enables dynamic holographic displays with ultra-high computational and display frame rates. The metasurface device was spatially divided into multiple different channel regions, each of which projects a reconstructed sub-pattern. The process of updating the hologram was mapped to bitwise operations on a set of bit values, thus avoiding any complex hologram computation during dynamic refresh. These bitwise operations not only enable efficient computation, but also facilitate the quick and simple construction of update masks for on-demand alterations, thereby significantly reducing computational demands. Our methodology requires very low computational power and can be executed even on low-power computing devices at high speed. On the Raspberry Pi computational platform as demonstrated, we measured a maximum computational frame rate of up to 800 kHz, and the DMD provided a maximum display frame rate of up to 23 kHz.

Furthermore, modern CPUs provide vectorized instructions, such as Single Instruction and Multiple Data (SIMD), which enable simultaneous operation on many bit values. Owing to the partitioned control and simplicity of image structure, our strategy can effectively utilize vectorized instructions and parallel programming techniques to further boost the efficiency of bitwise operations and image generation.

The unmodulated zero-order light observed in the experimental results can be eliminating through filtering, tailored device design, and refining hologram computation algorithms. Implementing these measures can significantly boost efficiency and improve the quality of the hologram. Detailed methods for eliminating zero-order light are described in the Supplementary information Section 6.

While the overall device in this study was primarily designed for the Tetris game, by strategically planning the basic meta-display patterns, our scheme has the potential to generate many complexes and undefined patterns on the fly with flexible and efficient dynamic control, promising candidate for building a general-purpose dynamic meta-holography system. Notably, our system allows for expanding more prosperous interaction methods, such as gesture control[34], further integrating the advantages of meta-holography with actual interaction. And it allows the extension to other multi-channel multiplexing technologies, such as OAM multiplexing, which, combined with the ultra-high computational frame rate characteristic of our Bit-MH, allows for more specific and specialized light field automation control, such as light-controlled array switches, spatial optical communications, optical computing, which can offer high-speed and flexible modulation capabilities for light field transformation.

Our proposed dynamic interactive bitwise meta-holography can inspire the related field, offering a practical and powerful approach for advanced human-computer interaction, real-time 3D visualization, and next-generation virtual and augmented reality systems, etc.

References

1. Xu K, Wang XE, Fan XH et al. Meta-holography: from concept to realization. *Opto-Electron Eng* **49**, 220183 (2022).
2. Horimai H, Tan XD. Holographic information storage system: today and future. *IEEE Trans Magn* **43**, 943–947 (2007).
3. Gao H, Fan XH, Xiong W et al. Recent advances in optical dynamic meta-holography. *Opto-Electron Adv* **4**, 210030 (2021).
4. Xiong JH, Hsiang EL, He ZQ et al. Augmented reality and virtual reality displays: emerging technologies and future perspectives. *Light Sci Appl* **10**, 216 (2021).
5. Fang XY, Ren HR, Gu M. Orbital angular momentum holography for high-security encryption. *Nat Photonics* **14**, 102–108 (2020).
6. Li JX, Kamin S, Zheng GX et al. Addressable metasurfaces for dynamic holography and optical information encryption. *Sci Adv* **4**, eaar6768 (2018).
7. Wu JC, Liu KX, Sui X et al. High-speed computer-generated holography using an autoencoder-based deep neural network. *Opt Lett* **46**, 2908–2911 (2021).
8. González H, Martínez-León L, Soldevila F et al. High sampling rate single-pixel digital holography system employing a DMD and phase-encoded patterns. *Opt Express* **26**, 20342–20350 (2018).
9. Gao H, Wang YX, Fan XH et al. Dynamic 3D meta-holography in visible range with large frame number and high frame rate. *Sci Adv* **6**, eaba8595 (2020).
10. Yu NF, Genevet P, Kats MA et al. Light propagation with phase discontinuities: generalized laws of reflection and refraction. *Science* **334**, 333–337 (2011).
11. Ni YB, Chen S, Wang YJ et al. Metasurface for structured light projection over 120° field of view. *Nano Lett* **20**, 6719–6724 (2020).
12. Mu YH, Zheng MY, Qi JR et al. A large field-of-view metasurface for complex-amplitude hologram breaking numerical aperture limitation. *Nanophotonics* **9**, 4749–4759 (2020).
13. Zhang YX, Pu MB, Jin JJ et al. Crosstalk-free achromatic full Stokes imaging polarimetry metasurface enabled by polarization-dependent phase optimization. *Opto-Electron Adv* **5**, 220058 (2022).
14. Guo XY, Zhong JZ, Li BJ et al. Full-color holographic display and encryption with full-polarization degree of freedom. *Adv Mater* **34**, 2103192 (2022).
15. Wang H, Ruan QF, Wang HT et al. Full color and grayscale painting with 3D printed low-index nanopillars. *Nano Lett* **21**, 4721–4729 (2021).
16. Dong FL, Chu WG. Multichannel-independent information encoding with optical metasurfaces. *Adv Mater* **31**, 1804921 (2019).
17. Zhao RZ, Huang LL, Wang YT. Recent advances in multi-dimensional metasurfaces holographic technologies. *PhotoniX* **1**, 20 (2020).
18. Zhang M, Pu MB, Zhang F et al. Plasmonic metasurfaces for switchable photonic spin–orbit interactions based on phase change materials. *Adv Sci* **5**, 1800835 (2018).
19. Choi C, Mun SE, Sung J et al. Hybrid state engineering of phase-change metasurface for all-optical cryptography. *Adv Funct Mater* **31**, 2007210 (2021).
20. Zeng C, Lu H, Mao D et al. Graphene-empowered dynamic metasurfaces and metadevices. *Opto-Electron Adv* **5**, 200098 (2022).
21. Wan CW, Li Z, Wan S et al. Electric-driven meta-optic dynamics for simultaneous near-/far-field multiplexing display. *Adv Funct Mater* **32**, 2110592 (2022).
22. Nemati A, Wang Q, Ang NSS et al. Ultra-high extinction-ratio light modulation by electrically tunable metasurface using dual epsilon-near-zero resonances. *Opto-Electron Adv* **4**, 200088 (2021).
23. Li TY, Wei QS, Reineke B et al. Reconfigurable metasurface hologram by utilizing addressable dynamic pixels. *Opt Express* **27**, 21153–21162 (2019).
24. Malek SC, Ee HS, Agarwal R. Strain multiplexed metasurface holograms on a stretchable substrate. *Nano Lett* **17**, 3641–3645 (2017).
25. Yang R, Wan S, Shi YY et al. Immersive tuning the guided waves for multifunctional on-chip metaoptics. *Laser Photonics Rev* **16**, 2200127 (2022).
26. Jang J, Lee GY, Sung J et al. Independent multichannel wavefront modulation for angle multiplexed meta-holograms. *Adv Opt Mater* **9**, 2100678 (2021).
27. Balthasar Mueller JP, Rubin NA, Devlin RC et al. Metasurface polarization optics: independent phase control of arbitrary orthogonal states of polarization. *Phys Rev Lett* **118**, 113901 (2017).
28. Li ZL, Chen C, Guan ZQ et al. Three-channel metasurfaces for simultaneous meta-holography and meta-nanoprinting: a single-cell design approach. *Laser Photonics Rev* **14**, 2000032 (2020).
29. Ren HR, Fang XY, Jang J et al. Complex-amplitude metasurface-based orbital angular momentum holography in momentum space. *Nat Nanotechnol* **15**, 948–955 (2020).
30. Masuda N, Ito T, Tanaka T et al. Computer generated holography using a graphics processing unit. *Opt Express* **14**, 603–608 (2006).
31. Yamamoto Y, Nakayama H, Takada N et al. Large-scale electroholography by HORN-8 from a point-cloud model with 400, 000 points. *Opt Express* **26**, 34259–34265 (2018).
32. Gerchberg RW. A practical algorithm for the determination of phase from image and diffraction plane pictures. *Optik* **35**, 237–246 (1972).
33. Li X, Chen QM, Zhang X et al. Time-sequential color code division multiplexing holographic display with metasurface. *Opto-Electron Adv* **6**, 220060 (2023).
34. Yamada S, Kakue T, Shimobaba T et al. Interactive holographic display based on finger gestures. *Sci Rep* **8**, 2010 (2018).

Acknowledgements

Author contributions

Y. C. Liu, X. H. Fan, H. Gao, W. Xiong conceived and designed the study; K. Xu designed and built the experimental system; Y. C. Liu designed the metaurface device and developed the control program; K. Xu performed the experiments and analyzed and processed the experimental data. All authors jointly participated in the analysis and discussion of experimental results and wrote the manuscript.

Competing interests

The authors declare no competing financial interests.

Supplementary information

Supplementary information for this paper is available at
https://doi.org/10.29026/oea.2024.230108

Scan for Article PDF